Corrosive Method for Co-W Films Based on Double Primary Batteries Principle

Yuliang Yang, Haipeng Lu, Dalin Wu, Yezun Sun

Abstract—**Cobalt-tungsten (Co-W) film is widely used as the protective layer on steel substrates because of its excellent properties. To further improve a certain aspect of such film, it was necessary to study the relationship between its structure and performance. Co-W film was prepared by electrodeposition and the film tungsten content changed by varying the duty cycle. Based on the single primary battery principle, it was difficult to show the film's microstructure, due to galvanic protection by the PCrNi$_3$MoVA steel substrate during the corrosion process. Thus, a new corrosive method for the Co-W film was proposed based on double primary batteries principle. Based on this method, corrosion effects with different tungsten contents and two corrosive methods were studied. The results showed that the corrosive method based on the double primary batteries principle successfully displayed the Co-W film structure and the effects of the wiping corrosive method better than the direct corrosive method.**

Index Terms—Co-W film, Single primary battery, Double primary batteries, Tungsten content, Direct corrosive method, Wiping corrosive method

I. Introduction

Material performance is closely related to its microstructure. Therefore, it is a meaningful goal to find a suitable method for displaying and observing the material's microstructure.

Due to the excellent properties of wear resistance, corrosion resistance, and high temperature oxidation resistance, cobalt-tungsten (Co-W) film is widely used as a protective layer on steel substrates in the industrial, military, and aerospace fields [1–5]. To further improve the performance of a certain aspect of Co-W films, it was necessary to study the relationship between its structure and performance, to control the structure to improve its performance.

In this study, Co-W film was used in the inner tube of a gun barrel to improve ablation resistance and PCrNi$_3$MoVA steel used as the electrodeposit substrate. However, the corrosion resistance of PCrNi$_3$MoVA steel substrate was weaker than that of Co-W film. When aqua regia is used to corrode cross-sections of Co-W film on the substrate, the steel substrate will protect the Co-W film for the single primary battery principle, resulting in the substrate being constantly eroded and the film cross-sectional morphology not displayed [6–9].

To solve the problems mentioned above, the outer surface of Co-W film was combined with a 2-mm thick copper plate that was more resistant to corrosion. When the film cross-sectional structure of the layers were corroded with aqua regia, the PCrNi3MoVA steel substrate, Co-W film, and Cu plate would constitute double primary batteries. Although the steel substrate is still corroded, the Co-W film was also corroded, such that the film structure was successfully displayed. To make te corrosion effects more obvious, this study also compared the corrosion effects of the direct corrosive and the wiping corrosive methods.

I. Co-W Film Prepared by Electrodeposition

A. Performance of Co-W alloy

The melting point of W is as high as 3410℃, which can improve the creep and wear resistance of as alloy at high temperature. When such an alloy is heated to 1000–1100℃, it still has high hardness and wear resistance. Co has excellent properties, such as high temperature, oxidation, thermal corrosion, and thermal fatigue resistances [10]. When the temperature is increased to 630℃, it still possesses a stable structure. Thus, an alloy formed by Co and W has excellent properties, such as oxidation, high temperature, and thermal fatigue resistances [11]. In addition, the Co-W alloy deposition process also has green, environment-friendly and energy-saving manufacturing characteristics.

B. Substrate Pretreatment

PCrNi$_3$MoVA steel with 40 x 13 x 4 mm in size was the substrate. Its components (mass%) were: C 0.30– 0.40%，Si 0.10–0.35%，Mn 0.25－0.50%，Mo 0.20－0.80%，Cr 0.50－1.20%，Ni 2.00－3.30%，V 0.10－0.25%，p≤0.15%, S≤0.15%.

The substrate surface was first ground successively with 400#, 800#, 1200#, 2000# sandpaper and washed with distilled water. Then, the sample was placed in a caustic washing solution composed of 70 g/L NaOH, 30 g/L Na_2CO_3, 60 g/L $Na_3PO_4 \cdot 12H_2O$, and 12 g/L Na_2SiO_3 at 80℃ to remove oil until the surface of the sample immersed in the solution was not hung. Finally, the substrate surface was activated by immersion in 10% sulfuric acid (by vol) for 2 min, washed in distilled water, and dried for later use.

Yuliang Yang is with Shijiazhuang Campus of Army Engineering University, No.97 Heping West Road, Shijiazhuang, Hebei, 050003, China (e-mail: yyl_liang@sina.com).

Haipeng Lu is with the Army Test and Training Base, Baicheng 137001 ， China (corresponding author to provide phone: 18633456205; e-mail: 18603266703@163.com).)

Dalin Wu is with Shijiazhuang Campus of Army Engineering University, No.97 Heping West Road, Shijiazhuang, Hebei, 050003, China (e-mail: dalinwu@163.com)

Yezun Sun is with 32382 Unit of PLA, 100071, China (e-mail: sunyixiao003@126.com)

C. Co-W Film Prepared by Electrodeposition

The electrodeposition test device is shown in Figure 1.

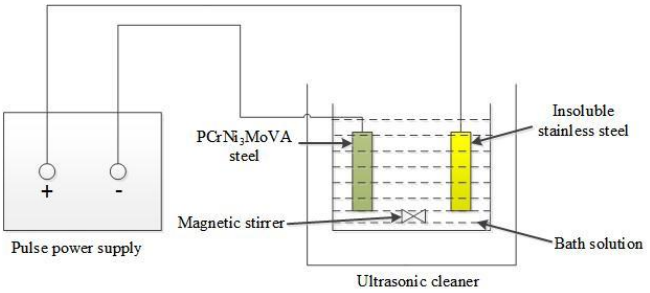

Fig. 1. Schematic of electrodeposition test device.

The anode was a 40 x 30 x 4 mm insoluble stainless steel plate and the cathode the $PCrNi_3MoVA$ steel substrate. The anode and cathode were connected to a SMD-30 type digitally-controlled double-pulse power supply. The bath formulation and basic process conditions were: 56.2 g/L $CoSO_4$ $7H_2O$, 66 g/L Na_2WO_4, 64.5 g/L $Na_2C_6H_5O_7$, 40 g/L H_3BO_3, 7.68 g/L $C_6H_8O_7$, at pH 6.7 ±0.1, 58 ℃, an average current density at 0.5 A/dm^2, and electrodeposition time of 50 minutes.

The pulse waveform generated by the pulse power supply is shown in Figure 2, where T_{on}, T_{off}, T, I_p, and I_a were the on-time, off-time, pulse period, limiting current density, and average current density, respectively. The duty cycle was expressed by $\lambda = T_{on} / T$.

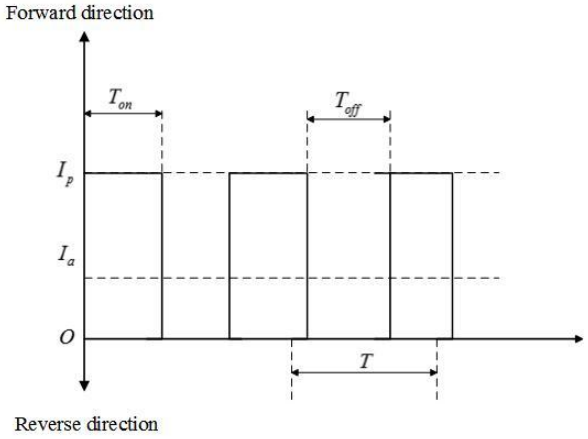

Fig. 2. Pulse waveform for producing Co-W film.

The W content in the film was changed by varying the duty cycle. Four types of Co-W films with different W contents were prepared under different duty cycles (Table I). The first type of Co-W film on a PCrNi3MoVA steel surface is shown in Figure 3.

TABLE I. *CO-W* FILMS WITH DIFFERENT TUNGSTEN CONTENT PREPARED UNDER DIFFERENT DUTY CYCLES

No.	Duty cycle (%)	W Content (at%)
1	100	7
2	60	11
3	30	13
4	10	17

Fig. 3. Co-W film, the surface of PCrNi3MoVA steel surface.

It can be seen that the film surface was uniform, flat and dense, without cracks, holes, burns, and burrs.

II. Cross-Sectional Morphology of Co-W Film after Corrosion by Direct Corrosive Method Based on the Single Primary Battery Principle

As Co-W film performance is closely related to its microstructure, it was a very meaningful to identify a suitable method for clearly displaying the microstructure.

A. Corrosive Methods of Co-W Film Cross-Sections

There are two common corrosive methods, including the direct corrosive and wiping methods.

The direct corrosive method involved immersing the section of a sample directly into a concave glass slide containing 5 ml of aqua regia and allowing 10 s of corrosive time. The wiping method was to use a cotton ball with aqua regia to wipe the corrosion for 5 times and each time was 2s.

B. Electrode Potential Calculation of Fe and Co-W

When aqua regia was used to corrode a C0-W cross-section, the $PCrNi_3MoVA$ steel substrate usually generated Fe^{3+} due to the strong oxidation of aqua regia, shown in equation 1. However, the generated Fe^{+3} continued to react with Fe to form Fe^{2+}, and Fe in the matrix reacted with hydrochloric acid to form Fe^{2+}. Therefore, the PCrNi3MoVA steel substrate eventually reacted as in equation 2 [12].

$$4HNO_3(aq) + Fe(s) = Fe(NO_3)_3(aq) + 2H_2O(l) + NO(g) \quad (1)$$

$$4HNO_3(aq) + 3Fe(s) + Fe(NO_3)_3(aq) + 2HCl(aq) = 2H_2O(l) + NO(g) + 3Fe(NO_3)_2(aq) + FeCl_2(aq) + H_2(g) \quad (2)$$

According to the Nernst equation, the electrode potential calculated corresponding to the electrode reaction $Fe + 2e^- = Fe^{2+}$ was

$$\varphi(Fe/Fe^{2+}) = \varphi^{\theta}\left(Fe/Fe^{2+}\right) + (RT/nF)\cdot\ln\left(1/C\left(Fe^{2+}\right)\right) = \varphi^{\theta}\left(Fe/Fe^{2+}\right) + (0.0592/n)\cdot\ln\left(1/C\left(Fe^{2+}\right)\right) = -0.440 - 0.0296\cdot\ln A$$

where, the T is 298.15K, R the gas constant, F the Faraday constant, n the number of electrons transferred in the electrode reaction, and φ^{θ} the standard electrode potential. Assuming that the concentration of Fe^{2+} was $C\left(Fe^{2+}\right) = A$ M.

If the *Co-W* film cross-section reacted with the aqua regia, the main component in the film was *Co*, such that the reaction was as shown in equation 3.

$$4HNO_3(aq) + 1.5Co(s) = 1.5Co(NO_3)_2(aq) + 2H_2O(l) + NO(g) \quad (3)$$

Assuming that the concentration of Co^{2+} after corrosion was the same as Fe^{2+}, the electrode potential corresponding to the electrode reaction $Co + 2e^- = Co^{2+}$ was calculated by the Nernst equation.

$$\varphi(Co/Co^{2+}) = \varphi^{\theta}\left(Co/Co^{2+}\right) + (RT/nF)\cdot\ln\left(1/C\left(Co^{2+}\right)\right)$$
$$= -0.220 - 0.0296\cdot\ln A$$

Therefore, $\varphi(Fe/Fe^{2+}) < \varphi(Co/Co^{2+})$.

C. Single Primary Battery Principle

When the cross-sectional structure of the Co-W film was corroded with aqua regia, the $PCrNi_3MoVA$ steel substrate and Co-W film constituted a single primary battery (Fig. 4).

Because of $\varphi(Fe/Fe^{2+}) < \varphi(Co/Co^{2+})$, the substrate of the film would protect the film from the galvanic cell, causing the substrate to be continuously corroded, and the *Co-W* film structure did not display the apparent microstructure.

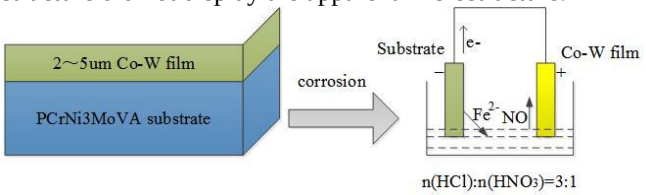

Fig. 4. Schematic of single primary battery.

D. Cross-Sectional Morphology of Co-W Film after Corrosion

The ultra-55 scanning electron microscopy with energy spectrometer was used to observe the cross-sectional morphology and elemental composition of the *Co-W* film (Fig. 5).

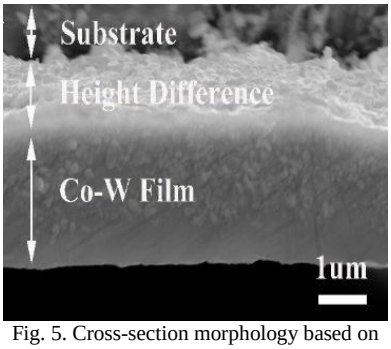

Fig. 5. Cross-section morphology based on single primary battery principle

From Fig. 5, No obvious microstructural morphology was observed in cross-sections of Co-W film and only some wear scars were after the polishing process.

III. Cross-Sectional Morphology of Co-W Film after Corrosion by the Direct Corrosive Method Based on the Double Primary Batteries Principle

A. Electrode Potential Calculation of Cu

If the copper plate reacted with aqua regia, assuming the concentration of Cu^{2+} after corrosion was the same as Fe^{2+}, the electrode potential corresponding to the electrode reaction $Cu + 2e^- = Cu^{2+}$ was calculated by the Nernst equation.

$$\varphi(Cu/Cu^{2+}) = \varphi^{\theta}\left(Cu/Cu^{2+}\right) + (RT/nF)\cdot\ln\left(1/C\left(Cu^{2+}\right)\right)$$
$$= 0.337 - 0.0296\cdot\ln A$$
$$4HNO_3(aq) + 1.5Cu(s) = 1.5Cu(NO_3)_2(aq) + 2H_2O(l) + NO(g) \quad (4)$$

Contrasting Fe and Co, the calculation results of the electrode potential was obtained, $\varphi(Fe/Fe^{2+}) < \varphi(Co/Co^{2+}) < \varphi(Cu/Cu^{2+})$.

Because the electrode potential of the three materials calculated by the Nernst equation were approximate, the open circuit potential of the three materials in aqua regia were tested and used to verify the corrosion resistance (Fig. 6).

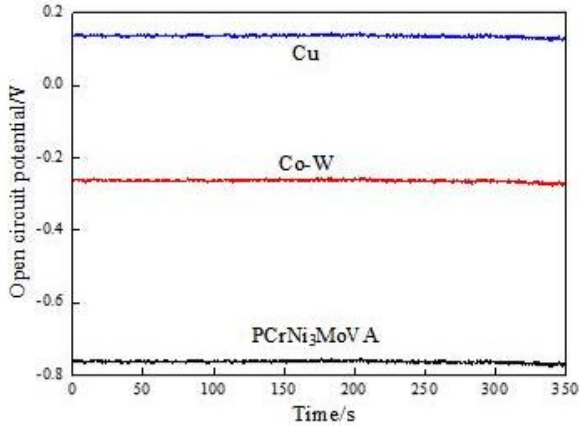

Fig. 6. Open circuit potential of Cu, Co-W, and PCrNi3MoVA steel in aqua regia.

The open circuit potential of the three materials in aqua regia was $PCrNi_3MoV$ < Co-W < $_{Cu}$, which indicated that the corrosion resistance of the three materials was PCrNi3MoV < Co-W < $_{Cu}$ (Fig. 6). The test results were consistent with the calculation results using the Nernst equation.

B. Double Primary Batteries Principle

When the cross-sectional structure of the Co-W film with a 2 mm thick copper plate was corroded with aqua regia, the $PCrNi_3MoVA$ steel substrate, Co-W film, and Cu plate constituted double primary batteries (Fig. 7).

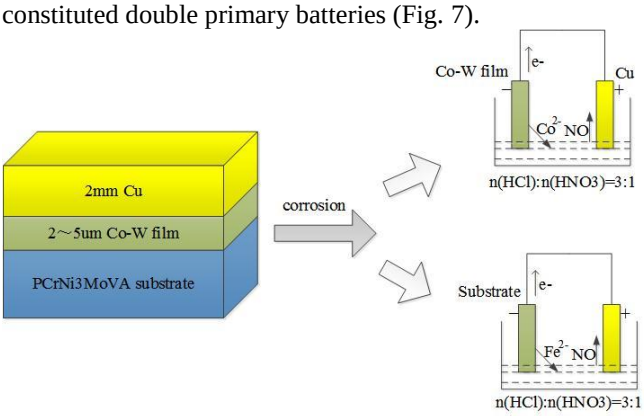

Fig. 7. Schematic of double primary batteries.

In the primary battery composed of the substrate and Co-W film, the substrate was used as the anode and Co-W film the cathode. In the primary battery composed of the copper plate and Co-W film, the film was used as the anode and the copper plate the cathode. Therefore, in the corrosion process, Co-W film was inevitably corroded, such that the film cross-sectional structure was revealed.

C. Cross-Sectional Morphology of Co-W Film after Corrosion by the Direct Corrosive Method

The actual corrosion effects on the Co-W film cross-sectional structure with W content of 7 at% based on the double primary batteries principle were shown in Figure 8 and the cross-sectional structure of the Co-W film was clearly shown. The grain structure was columnar and the film

structure near the substrate fine toothed, which indicated that the method was simple and effective.

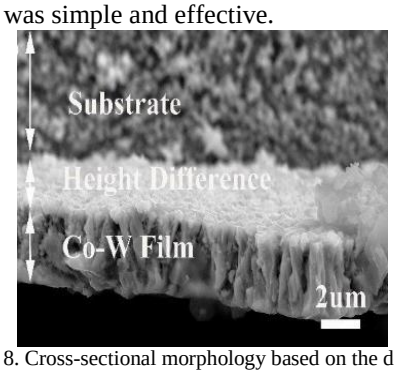

Fig. 8. Cross-sectional morphology based on the double primary batteries principle, 7 at% *W*.

D. Corrosive Effects with Different Tungsten Contents

The microstructure of the Co-W films with the three higher W contents (11, 13, and 17 at%) are shown from Figures 9–11, respectively.

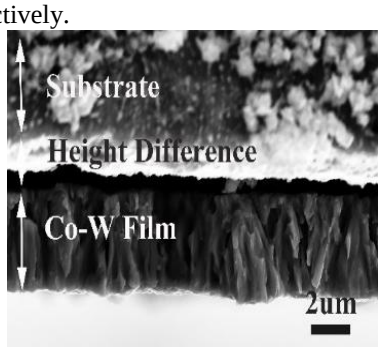

Fig. 9. Cross-sectional morphology based on the double primary batteries principle, 11at% *W*.

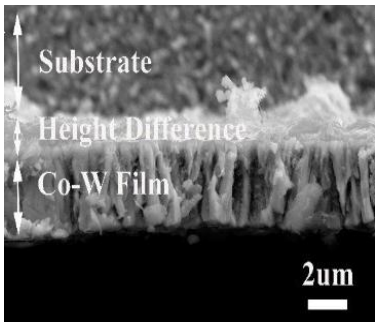

Fig. 10. Cross-sectional morphology based on the double primary batteries principle, 13at% *W*.

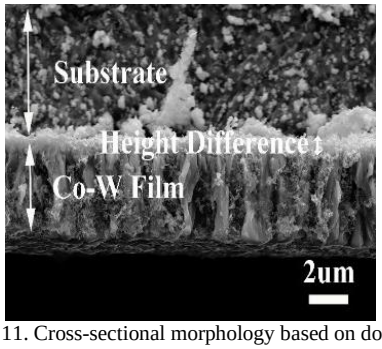

Fig. 11. Cross-sectional morphology based on double primary batteries principle, 17at% *W*.

Compared with 7 at% W (Fig. 6), the microstructures of higher W films were clearly visible (Figs. 9–11), indicating that this method was not only applicable to low W content but also to higher contents.

IV. Cross-Sectional Morphology after Corrosion by the Wiping Corrosive Method Based on the Double Primary Batteries Principle

It was observed in Figures 5 and 9–11 that there were differences in height between the film and substrate. This affected the observations of film structure. The cross-sectional morphology after corrosion by the wiping corrosive method is shown in Figure 12.

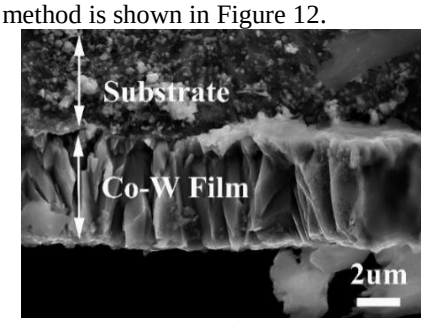

Fig. 12. *Cross-sectional morphology after corrosion by the wipe corrosive method.*

From Fig. 12, The cross-sectional microstructure of Co-W film obtained by the wiping corrosive method was clear and discernible and there were basically no height differences between the film and the substrate.

V. Conclusions

(1) Co-W films were prepared by electrodeposition and the W content in the film changed by varying the duty cycle.

(2) The electrode potentials of three materials were calculated using the Nernst equation, $\varphi(Fe/Fe^{2+}) < \varphi(Co/Co^{2+}) < \varphi(Cu/Cu^{2+})$, were consistent with test results.

(3) The corrosive method based on the single primary battery principle was difficult for displaying Co-W film microstructure due to galvanic protection effects of the substrate during the corrosion process.

(4) The corrosive method based on the double primary batteries principle was not only suitable for cross-sectional corrosion of Co-W film with low W content but also with high W content.

(5) The cross-sectional microstructures of Co-W films obtained by the wiping corrosive method were not only clear and identifiable but also showed no great differences between the corroded film and substrate. Thus, corrosion effects were better than that from the direct corrosive method.

References

[1] D. P. Weston, P. H. Shipway, S. J. Harris and M. K. Chen, "Friction and sliding wear behavior of electrodeposited cobalt and cobalt-tungstent alloy coatings for replacement of electrodeposited chromium," Wear, vol. 267, no. 5-8, pp. 934–943, Jun. 2009.

[2] D.P. Weston, S. J. Harris, H. Capel, N. Ahmed, P. H. Shipway and J.M. Yellup, "Nanostructured Co–W coatings produced by electrodeposition to replace hard Cr on aerospace components," Trans of the IMF, vol. 88, no. 1, pp. 47–56, Jul. 2013.

[3] Z. Ghaferi, K. Raeissi, M. A. Golozar and H. Edris, "Characterization of nanocrystalline Co–W coatings on Cu substrate, electrodeposited from a citrate-ammonia bath," Surface and coating technology, vol. 26, no.2, pp. 495-505, 2011.

[4] Feyisayo V. Adams, Anuoluwapo T. Bankole, O'Donnell P. Sylvester, Ayodeji O. Apata, Ifeoma V. Joseph, and Onoyivwe M. Ama, "Corrosion Behavior of Ferritic Stainless Steel in Locally Prepared Biodiesel Media," Lecture Notes in Engineering and Computer Science: Proceedings of The World Congress on Engineering 2018, 4-6 July, 2018, London, U.K., pp462-466.

[5] George I. Ononiwu, Feyisayo V. Adams, Ifeoma V. Joseph, and Ayo S. Afolabi, "Corrosion Behaviour of Mild Steel in Biodiesel Prepared from Ghee Butter," Lecture Notes in Engineering and Computer Science: Proceedings of The World Congress on Engineering 2015, 1-3 July, 2015, London, U.K., pp858-862.

[6] Yin-Hsien Su, Tai-Chen Kou, Wen-His Lee, Yu-Sheng Wang, Chi-Cheng Hung, Wei-Hsiang Tseng, Kuo-Hsiu Wei, Ying-Lang Wang, "Effect of tungsten incorporation in cobalt tungsten alloys as seedless diffusion barrier materials," Microelectronic Engineering, vol. 171, pp. 25-30, Mar. 2017.

[7] Mrinalini Mulukutla, Vamsi Karthik Kommineni, Sandip P. Harimkar, "Pulsed electrodeposition of Co–W amorphous and crystalline coatings," Applied Surface Science, vol. 258, no.7, pp. 2886-2893, Jan.2012.

[8] Fenghua Su, Cansen Liu and Ping Huang, "Establishing Relationships between Electrodeposition Techniques, Microstructure and Properties of Nanocrystalline Co–W Aloy Coatings," Journal of Alloys and Compounds, vol. 557, pp. 228-238, Apr. 2013.

[9] N. Fathollahzade and K. Raeissi. Electrochemical evaluation of corrosion and tribo-corrosion behavior of amorphous and nanocrystalline cobalt-tungstent electrodeposited coatings," Materials Chemistry and Physics, vol. 148, pp. 67-76, Aug. 2014.

[10] Tong Y X, Liu P, Liu L Z. Electrochemical behaviors of Fe2+ and Sm3+ in Urea-Na Br low temperaturemelt and their induced code-position [J]. Journal of Rare Earths, 2001, 19(4): 275-279.

[11] K L Narayana, and M Kedar Mallik, "Comparison of Properties of Laser Deposited Co-Cr-Mo and Co-Cr-W Alloys," Lecture Notes in Engineering and Computer Science: Proceedings of The World Congress on Engineering 2019, 3-5 July, 2019, London, U.K., pp406-409

[12] Mei Yang and Liang Xian, "The Calculation of Reduction Electrode Potential with Nernst Equation in Multiple Chemical Reaction Equilibrium", Journal of Northwest University for Nationalities(Natural Science), vol. 19, no.110, pp. 10-12, Jul. 2018.